

Ophthalmic Laser Therapy: Mechanisms and Applications

Daniel Palanker

Department of Ophthalmology and Hansen Experimental Physics Laboratory,
Stanford University, Stanford, CA

Definition

The term **LASER** is an abbreviation which stands for **L**ight **A**mplification by **S**timulated **E**mission of **R**adiation. The laser is a source of coherent, directional, monochromatic light that can be precisely focused into a small spot. The laser is a very useful tool for a wide variety of clinical diagnostic and therapeutic procedures.

Principles of Light Emission by Lasers

Molecules are made up of atoms, which are composed of a positively charged nucleus and negatively charged electrons orbiting it at various energy levels. Light is composed of individual packets of energy, called photons. Electrons can jump from one orbit to another by either, absorbing energy and moving to a higher level (excited state), or emitting energy and transitioning to a lower level. Such transitions can be accompanied by absorption or spontaneous emission of a **photon**.

“**Stimulated Emission**” is a process in which photon emission is stimulated by interaction of an atom in excited state with a passing photon. The photon emitted by the atom in this process will have the same phase, direction of propagation and wavelength as the “stimulating photon”. The “stimulating photon” does not lose energy during this interaction- it simply causes the emission and continues on, as illustrated in Figure 1.

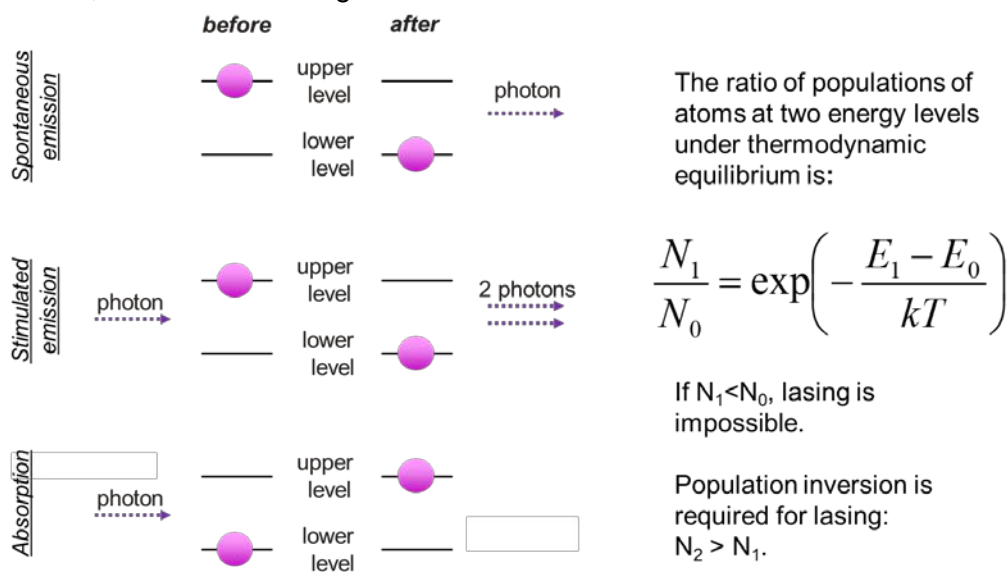
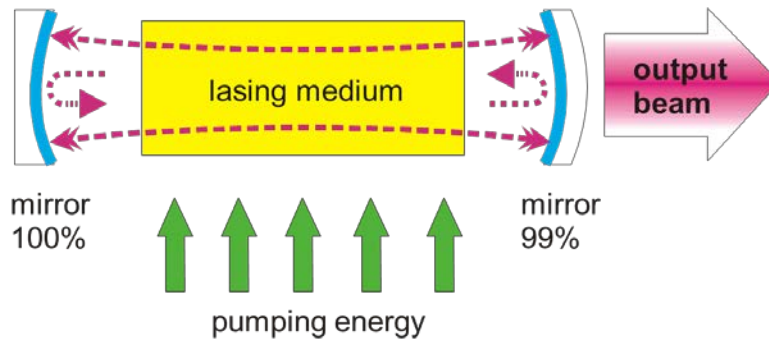


Figure 1: LASER: Light Amplification by Stimulated Emission of Radiation

For such stimulated emission to occur more frequently than absorption (and hence result in light amplification), the optical material should have more atoms in excited state than in a lower state. Such “inversion of population” can be achieved in some materials using an excitation source, or “pump”. Another essential element of the laser is an optical cavity which circulates the emitted light between the two mirrors, with a fraction of the photons escaping through the front mirror to form the laser beam. The light trapped inside the cavity stimulates emission of new photons from the excited laser material with the same wavelength, direction and phase, thereby forming a coherent laser beam, as illustrated in Figure 2.



Placing mirrors at opposite ends of a laser cavity enables the beam to travel back and forth, leading to increased amplification due to the longer path length through the medium. The multiple reflections also produce a very directional beam because only photons traveling along the cavity axis will be reflected from both mirrors.

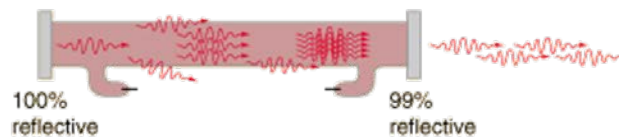


Figure 2: Structure of a Laser

High directionality of the laser beam allows for tight focusing. Monochromaticity of light beam helps avoiding chromatic aberration in the optical system, and allows for selective targeting of the tissue absorption spectrum.

Basic Instrument Design

The lasing medium is contained in an optical cavity (resonator) with mirrors at both ends, which reflect the light into the cavity and thereby circulate the photons through the lasing material multiple times to efficiently stimulate emission of radiation from excited atoms. One of the mirrors is partially transmitting, thereby allowing a fraction of the laser beam to emerge. The lasing (or gain) medium can be a gas, liquid, or solid. Lasers can be pumped by continuous discharge lamps and by pulsed flash lamps, by electric discharges in the laser medium, by chemical reactions, by an electron beam, by direct conversion of electric current into photons in semiconductors, or by light from other lasers. Laser pulse durations can vary from femtoseconds to infinity (continuous wave). Pulsing techniques used for different ranges of pulse durations include electronic shutters (down to 1 ms), pulsed flash lamps (typically down to a few μ s), Q-switching (down to a few ns), or mode-locking (down to fs).

Electromagnetic Spectrum

Wavelength range of ophthalmic lasers extends from 193nm to 10800nm, including the visible spectrum: approximately between 400 and 750 nm (see Table 1).

Laser type	Wavelength	Typical pulse duration	Interaction
CO ₂	9.2 - 10.8 μm	CW or ms pulsed	thermal
Er:YAG	2.94 μm	100 ns – 250 μs	thermal + mechanical
Er:YSGG	2.78 μm	100 ns – 250 μs	thermal + mechanical
Ho:YAG	2.12 μm	100 ns – 250 μs	thermal + mechanical
Nd:YAG	1064 nm ($\lambda/2=532\text{nm}$)	100 ps - CW	plasma+thermal+mech
Nd:YLF	1053 nm ($\lambda/2=526\text{nm}$)	1 ps - CW	plasma+thermal+mech
Ti:Sapphire	700-1000 nm	60 fs – 10 ps	plasma
Diode	635 – 1550 nm	Few ns - CW	thermal + photochem
Alexandrite	720 – 800 nm	50 ns – 100 μs	thermal
Ruby	694 nm	1-250 μs	thermal
Krypton ion	531, 568, 647 nm	CW or ms pulsed	thermal
HeNe	633 nm	CW	imaging
Argon ion	488, 514 nm	CW or ms pulsed	thermal
ArF excimer	193 nm	3-20 ns	photoablation

Table 1. Common medical lasers

The shorter the wavelength, the higher is the photon frequency and its energy. Sufficiently high energy (deep ultraviolet) photons can dissociate molecules and ionize atoms. Visible range photons can excite electrons and initiate photochemical reactions, while the infrared wavelengths can interact with vibrational and rotational degrees of freedom in molecules, eventually leading to tissue heating. Absorption spectra of the major ocular chromophores, including water, oxy- and deoxy-hemoglobin, melanin and xanthophyll, are shown in Figure 3.

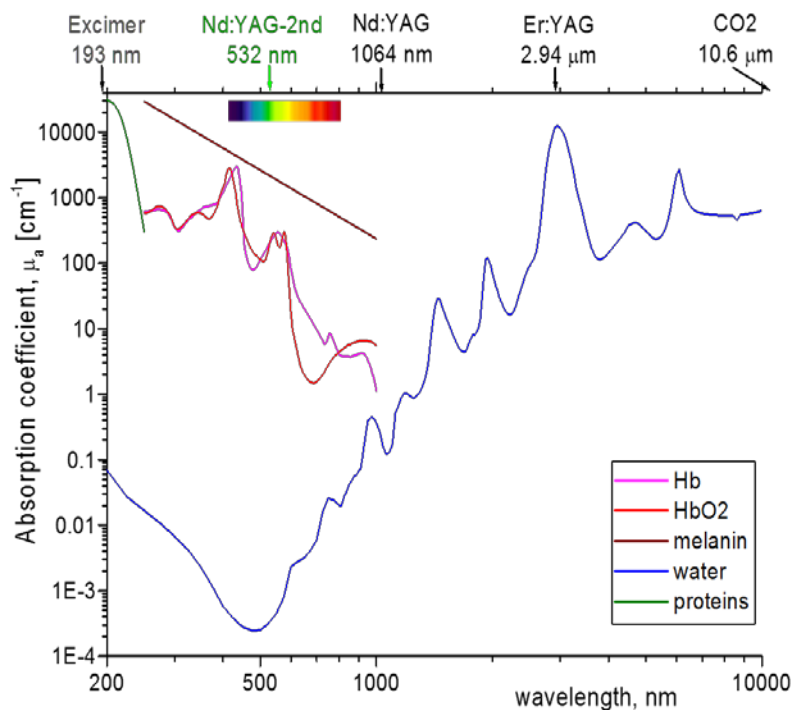


Figure 3A: Absorption spectra of the major ocular chromophores.

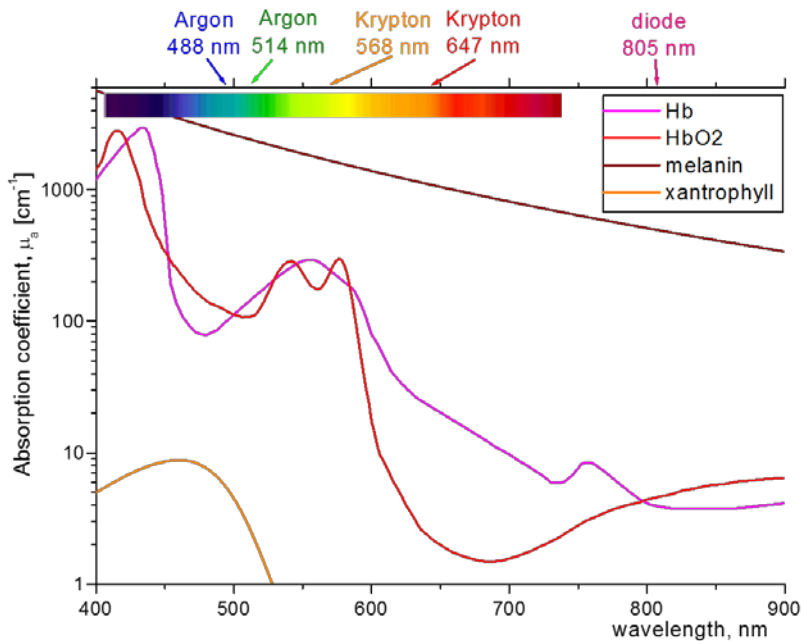


Figure 3B: Absorption spectra of the major ocular chromophores in the visible part of the spectrum, including Hemoglobin, Melanin and Xanthophyll

Laser beam delivery to tissue

Laser beams are typically very well collimated, i.e. the photons propagate within a very narrow angular spread. [Diffraction](#) causes light waves to spread transversely as they propagate, and it is therefore impossible to have a perfectly collimated beam. The diffraction-limited divergence angle of a [Gaussian beam](#) with diameter D and wavelength λ is: $\Theta = \frac{4 \cdot \lambda}{\pi \cdot D}$.

As an example, for an Argon laser emitting a 1 mm wide beam at 515 nm wavelength, the divergence (half-angle Θ) is about 0.66 mrad, i.e. the beam spreads by 1.3 mm over a distance of 1 meter.

Using a lens or a concave mirror with focal length f , a laser beam can be focused to a spot with a diameter $d = \frac{4 \cdot f}{\pi \cdot D} \lambda$. The depth of the focal region is: $F = \frac{8 \cdot f^2}{\pi \cdot D^2} \lambda$ (see Figure 4).

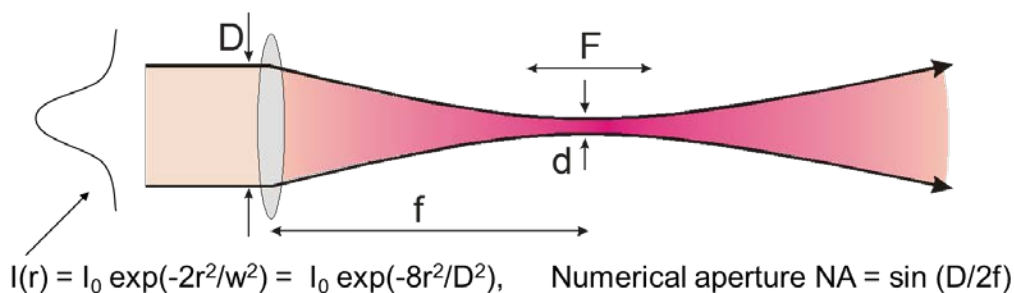


Figure 4: Focusing of the free-propagating laser beam.

With a lens of a focal length $f=25$ mm the same Argon laser beam can be focused to a spot of $16\ \mu\text{m}$ in diameter, having a focal depth of $820\ \mu\text{m}$. It must be kept in mind though that exact definition of the spot size depends on the beam profile, which varies in various configurations of laser cavities.

As an alternative to a free-propagating beam, laser light can be transported via [optical fibers](#). An optical fiber, schematically shown in Figure 5, typically consists of a core, cladding and jacket. Light is trapped within the core due to the [total internal reflection](#) at the interface of the core with cladding. To satisfy conditions of total internal reflection, the incidence angle of light at the core/cladding interface should not exceed the critical angle of total internal reflection: $\sin\Theta_{cr}=n_{core}/n_{clad}$, where n_{core} and n_{clad} are refractive indices of the core and cladding, respectively. To satisfy these criteria for total internal reflection, the light should be launched within a so called acceptance cone, and the sine of its half-angle Θ_{ac} is defined as the Numerical Aperture of the fiber: $NA = \sin\Theta_{ac} = \sqrt{n_{core}^2 - n_{clad}^2}$. Typically the NA is within a range of 0.1 - 0.2. Optical fibers are often used for delivery of laser light to slit lamp-based systems, and to the intraocular surgical probes.

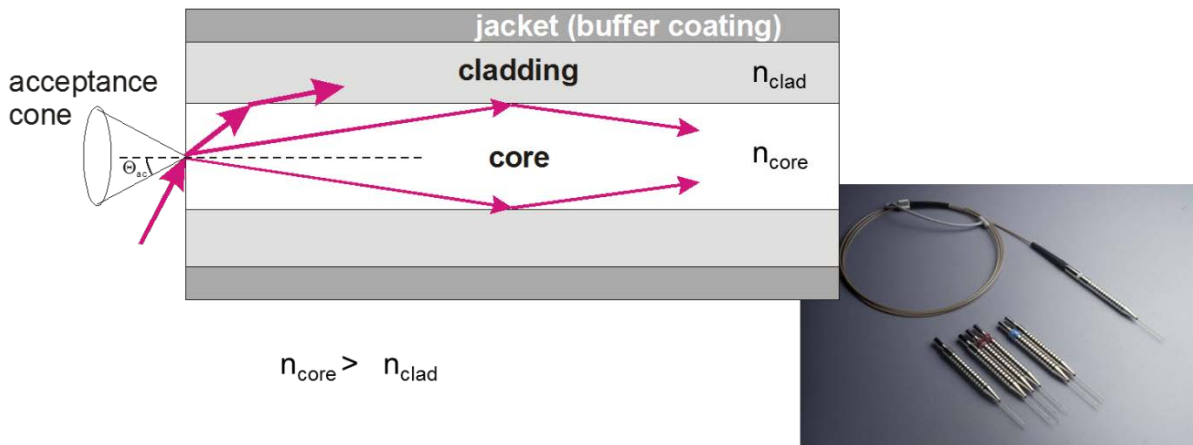


Figure 5: Fiber delivery of the laser beam

Laser-Tissue Interactions

Interactions of light with biological tissues depend on its wavelength, pulse duration and irradiance (amount of power per unit area, W/cm^2). With sufficiently high photon energy (i.e. short wavelength) light can induce photochemical reactions. Light absorption by the tissue can also result in heating, which may lead to thermal denaturation. At higher temperatures, and especially with shorter pulses, tissue can be rapidly vaporized, which can result in mechanical disruption or ejection of tissue fragments. Very short pulses with high peak irradiance can ionize materials, enabling dissection inside transparent tissues. These interactions are described below in more detail.

Photochemical Interactions

Light-induced chemical reactions, such as photo-transduction in photoreceptors initiated by the light-induced isomerization of 11-cis retinal to all-trans retinal, are typically not associated with a meaningful change in tissue temperature. In addition to the natural chromophores, like rhodopsin, such interactions can be mediated by exogenously administered agents, such as verteporfin[1]. Photochemical interactions are the basis for retinal photodynamic therapy (PDT) in age related macular degeneration, or cross linking of corneal collagen with riboflavin to treat keratoconus. To avoid heating, therapeutic photochemical interactions are typically performed at very low irradiances ($<1\ \text{W}/\text{cm}^2$) and with long exposures - tens of seconds[2].

In the case of retinal PDT, absorption of a photon of specific wavelength by the porphyrin molecule (photosensitizer) transitions it into the singlet excited state ($^1P^*$). It can then either decay back to the ground state, or it can be converted into the triplet excited state ($^3P^*$), which is able to transfer energy to a triplet ground state of oxygen. Such energy transfer results in highly toxic singlet oxygen (1O_2)

which can produce irreversible oxidation of the cell structures in the areas of selective accumulation of the administered photosensitizer, for example in the newly forming blood vessels[3].

Photo-thermal Interactions

Temperature is the governing parameter in all thermal laser-tissue interactions. Depending on the temperature rise and duration of exposure, different tissue effects may occur, including necrosis, coagulation and vaporization. Absorption coefficient of the tissue chromophores strongly depends on the wavelength. Major chromophores of ocular tissues include water (for infrared wavelengths), proteins (for deep UV), melanin, blood, and macular pigments (for visible wavelengths). The extent of tissue damage can be quantified by the decline in concentration of a critical molecular component for cellular metabolism as a function of temperature and duration of exposure [4, 5]. The Arrhenius integral-based quantification of the tissue damage assumes that irreversible effects takes place when the concentration of a critical molecular component of the treated tissue drops below some threshold value. Conventionally, an Arrhenius integral of unity corresponds to a reduction in concentration by 63% ($1/e$) of a critical molecular component that has been damaged.

If heat diffusion is not taken into account, then at a constant beam intensity the temperature rises linearly with time. The role of heat diffusion during the laser pulse becomes significant when the pulse duration exceeds the time it takes for heat to spread over the distance equal to the laser penetration depth (or initial heat deposition zone) in tissue. This characteristic duration of diffusion scales with the square of the characteristic length. For example, for a $1\mu\text{m}$ -size object (e.g. melanosome) in water the characteristic heat diffusion time is about $1.7\ \mu\text{s}$, while for 1 mm the diffusion time is about 1.7 seconds. For pulses shorter than the characteristic diffusion time across the light absorption zone, the heat cannot escape from the energy deposition zone during the pulse, which results in the most efficient heating – a condition called “heat confinement”.

Retinal Photocoagulation

Retinal photocoagulation typically involves application of laser pulses with durations ranging from 10 to 200ms, and transient hyperthermia by tens of degrees Celsius above body temperature. Various lasers have been used in the past (Ruby (694 nm), Argon (488, 514 nm), Krypton (647 nm)). Currently the most common lasers in photocoagulation are frequency-doubled Nd:YAG (532 nm), and yellow semiconductor laser (577nm). The laser energy is absorbed primarily by melanin in the RPE and choroid, and by hemoglobin. At a 532 nm wavelength approximately 5% of light incident on the retina is absorbed by neural retina, about half is absorbed in the RPE, and the rest in the choroid[4] (Figure 6).

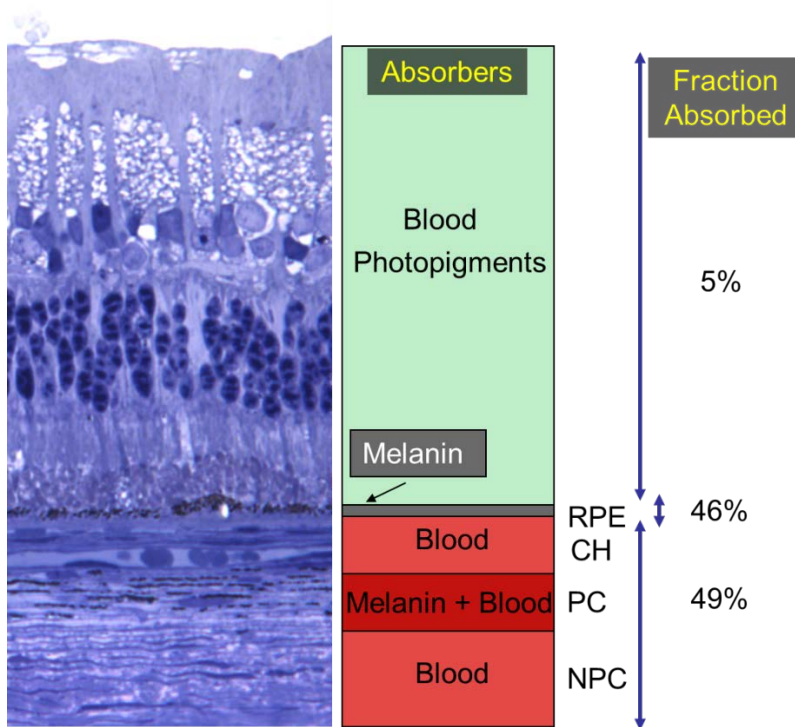


Figure 6. Histology of the rabbit retina, with major chromophores, and the fraction of the laser beam absorbed in various retinal layers. CH- choriocapillaris, PC – pigmented choroid, NPC – non-pigmented choroid.

Heat generated by light absorption in RPE and choroid diffuses into the retina and causes coagulation of the photoreceptors and, sometimes, of the inner retina. During 100ms applications, the heat diffuses up to 200 μm into the retina, thus “smoothing” the edge and extending the coagulated zone beyond the boundaries of the laser spot, termed “thermal blooming”. Heat diffusion using shorter pulses and smaller spot sizes can be limited to the photoreceptor layer, thereby avoiding or minimizing inner retinal damage. The width of the retinal lesion increases linearly with laser power and logarithmically with pulse duration (Figure 7).

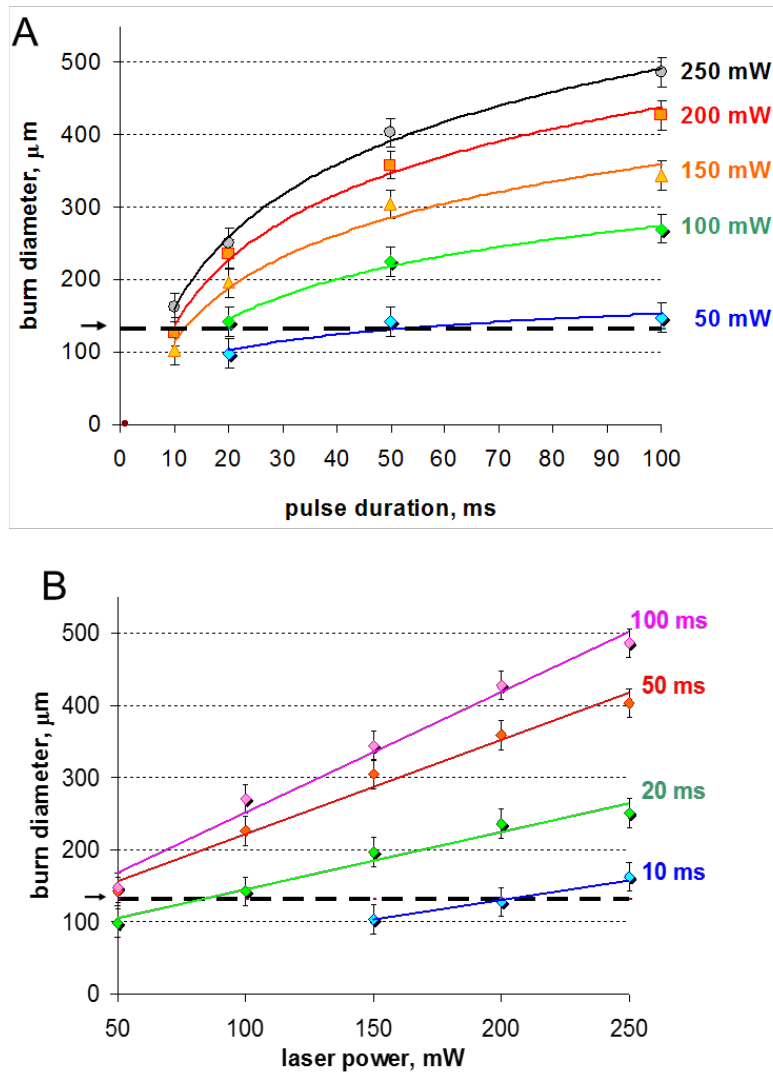


Figure 7: Lesion diameters for 132µm beam size in rabbit retina as a function of pulse duration (A) and power (B).

The threshold power required for creation of the retinal lesion increases with decreasing pulse duration, as illustrated in Figure 8A for a 132 µm retinal laser spot in the rabbit eye. For pulse durations of 20, 50, and 100 ms all clinical grades (mild, moderate, intense, very intense, and rupture) can be created with the appropriate choice of power settings. At pulse durations below 10 ms, it became increasingly difficult to reproducibly create moderate to intense lesions without inadvertently rupturing the retina. At 2 ms or less it is not possible to consistently create a moderate lesion without rupturing the retina.

The ratio of the threshold power required for producing a rupture to that required for producing a mild lesion is defined as the therapeutic window, and represents one means of quantifying the relative safety (dynamic range) of retinal photocoagulation. The larger this ratio the greater the margin of safety to create a visible lesion without inadvertently inducing a retinal rupture. Figure 8B depicts the width of this therapeutic window as a function of pulse duration for two different laser spot sizes. With both spot sizes, the therapeutic window decreases to unity as pulse durations decrease to 1 ms. At this point there is effectively no safe range for visible retinal photocoagulation: mild lesion and rupture are equally likely to occur at the same power. The width of a safe therapeutic window should suffice to accommodate for variations in fundus pigmentation.

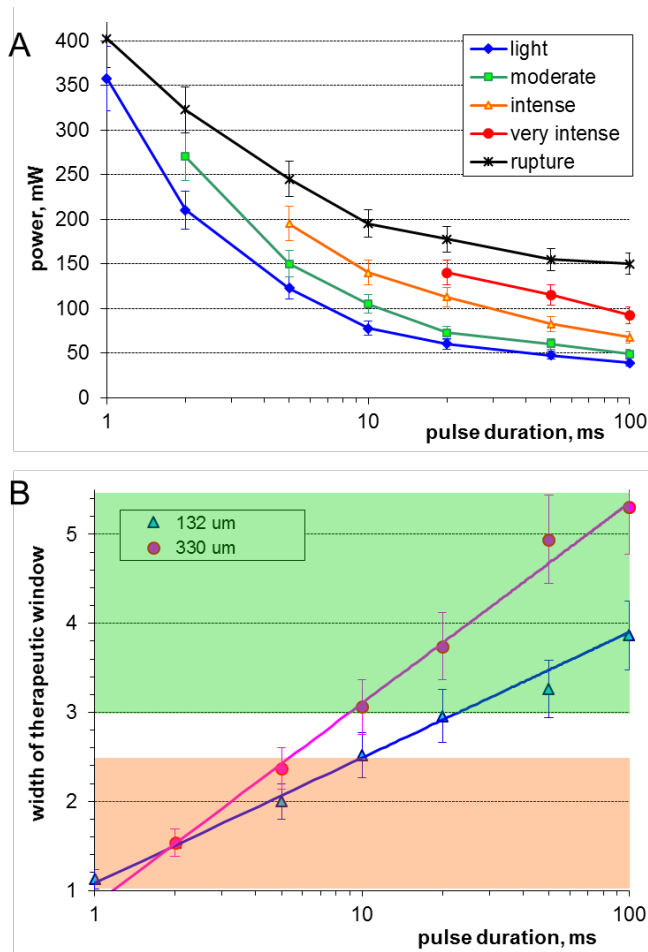


Figure 8: Lesion diameters for 132µm beam size in rabbit retina as a function of pulse duration (A) and power (B). C. Threshold power for lesions of various clinical grades, plotted as a function of pulse duration. D. Width of the safe therapeutic window for light coagulation, as a function of pulse duration for 132 µm and 330µm beam on the retina.

Photomechanical Interactions

Photomechanical interactions are at the heart of LASIK and other types of corneal refractive surgery. Precise corneal photoablation is achieved using nanosecond pulses of ArF excimer laser as a result of the limited 200 nm penetration depth of the 193nm radiation in the cornea and very short pulse durations (~10ns) enabling extremely precise ablation, with very narrow zone of the residual tissue damage (<0.2 µm) at the edges of the ablation zone.

Photoablation and photodisruption occur when laser absorption results in the tissue temperature exceeding the vaporization threshold. Expanding and collapsing vapor bubbles following explosive vaporization can rupture nearby tissue or eject tissue fragments from the exposed surface. Vaporization temperature ranges between 100 and 305 °C depending upon the pulse duration and on presence of the bubble nucleation sites. To avoid heat diffusion away from the laser absorption zone during the pulse, energy needs be delivered within the thermal confinement time accounting for the use of relatively short pulse durations - in the range of microseconds to nanoseconds rather than milliseconds[6].

Dielectric breakdown

Even though transparent tissue does not exhibit significant absorption in its wavelength range of transparency at extremely high irradiances (10^8 - 10^{11} W/cm²), which can be achieved in a tightly focused short-pulsed (ns-fs) laser beam, the electric field is so high that transparent material can be ionized[7]. This mechanism, called dielectric breakdown, allows for a highly localized deposition

of energy in the middle of a transparent medium – at the focal point of the laser beam. The development of plasma and associated absorption of the laser energy in the focal spot lead to explosive vaporization of the liquid medium, accompanied by the tissue rupture. (Figure 6)

Plasma-mediated laser-tissue interactions are applied to fragmentation of the opacified posterior lens capsule (secondary cataract) with nanosecond Nd:YAG lasers. At shorter pulse durations (1ps - 100 fs) and much lower energies ($\sim\mu\text{J}$) this process is applied to intrastromal cutting and formation of a corneal flap for refractive surgery[8, 9]. This approach has also been tested in the dissection of epiretinal membranes using a tightly focused beam[10]. Despite the very low energy required for this process (several μJ) its applicability in the posterior pole is limited due to the difficulty in axial differentiation between the epiretinal membranes and the retina located very close behind them. In addition, strong optical aberrations in the periphery of the posterior pole preclude tight focusing of the laser beam in these areas. Recently, this process has been applied to anterior capsulotomy and fragmentation of the crystalline lens during cataract surgery[11, 12].

Common Ophthalmic Laser Procedures

Retinal Photocoagulation

Retinal photocoagulation typically involves the application of laser pulses with durations ranging from 10 to 200ms, and transient hyperthermia by tens of degrees above body temperature. Various lasers have been used in the past (Ruby (694 nm), Argon (488, 514 nm), Krypton (647 nm)). Currently the most common lasers in photocoagulation are frequency-doubled Nd:YAG (532 nm), and yellow semiconductor laser (577nm). The laser energy is absorbed primarily by melanin in the RPE and choroid, and by hemoglobin in blood. At a 532 nm wavelength approximately half of the laser energy incident on the retina is absorbed in the RPE, and the rest in the choroid[4], as illustrated in Figure 6. The heat generated diffuses from the RPE and choroid into the retina and causes coagulation of the photoreceptors and, sometimes, of the inner retina. During 100ms applications, the heat diffuses distances of up to 200 μm thus “smoothing” the edge and extending the coagulated zone beyond the boundaries of the laser spot, termed “thermal blooming”. Heat diffusion using shorter pulses and with smaller spot sizes can be limited to the photoreceptor layer, thereby avoiding the inner retinal damage.

The threshold power required for the creation of retinal lesions increases with shorter pulses, since higher temperatures are required for coagulation during shorter exposures. The ratio of the threshold power required to produce a rupture to that required to produce a mild lesion is defined as the therapeutic window, and represents one means of quantifying the relative safety (dynamic range) of retinal photocoagulation. The larger this ratio the greater the margin of safety to create a visible lesion without inadvertently inducing a retinal rupture. Figure 8B depicts the width of this therapeutic window as a function of pulse duration for two different laser spot sizes. The width of the safe therapeutic window should suffice to accommodate for variations in fundus pigmentation, which typically do not exceed a factor of 2. To provide a safe therapeutic window larger than 2.5, pulse durations should equal or preferably exceed 10 ms for a beam of 330 μm , and 20 ms for the 132 μm spot size.

It is important to keep in mind that coagulation of blood vessels requires more energy than other tissue due to cooling by the blood flow. For example, if a spot size of 200 μm with exposure time of 200 ms is applied to occlude a blood vessel with flow velocity of 5 mm/s, the laser energy is effectively distributed over the column 5 times longer than the diameter of the laser spot. Thus the effective energy remaining at the photocoagulation site is 5 times lower than it would be in stationary tissue.

Pattern Scanning Laser Photocoagulation

The first attempts to make photocoagulation a completely automated procedure involved rather complex equipment, including image recognition software and eye tracking[13]. The complexity of such systems prevented their commercial introduction and acceptance in clinical practice.

A semi-automatic pattern scanning photocoagulator (PASCAL, Topcon Medical Laser Systems Inc.) was introduced by OptiMedica Corp. in 2005[14]. It delivered patterns of laser spots ranging from a single spot to 56 spots applied in a rapid sequence with a single depression of a foot pedal. The control of laser parameters was performed by means of a touch screen graphic user interface, facilitating selection of the different patterns of photocoagulation. The laser was activated by pressing a foot pedal, which was kept depressed until the entire pattern was completed. Although it is possible for the physician to release the foot pedal and stop the laser at will, prior to completion of the pattern, if clinically indicated.

Patterns included square arrays with up to 5x5 spots, arcs with the number of concentric rows varying from 1 to 3, circular patterns for photocoagulation of small holes and other lesions in the retinal periphery. Patterns for macular photocoagulation included rings and arcs with adjustable central exclusion zone of up to 2 mm in diameter to allow for laser application reducing the risk of inadvertent damage to the foveal avascular zone.

To deliver the whole pattern within the eye fixation time and avoid beam movement due to the ocular muscles, each exposure was required to be shorter than in conventional photocoagulation: 10-20 ms instead of 100-200 ms, traditionally applied with single spot exposures. Reduced heat diffusion into choroid during shorter exposures also resulted in patients experiencing less pain[15-17]. Short pulse lesions appear smaller and lighter than conventional burns produced with the same beam size, and therefore a larger number of them are required to treat the same total area[18].

An automatic laser delivery, guided by diagnostic imaging and stabilized using eye tracking, has been recently introduced in a Navilase™ system (OD-OS GmbH). This system includes retinal image acquisition, annotation of the images to create a detailed treatment plan, and then automated delivery of the laser to the retina according to the treatment plan.

Clinical Indications: Treatment of Diabetic Retinopathy

Photocoagulation has proven safe and effective in the treatment of proliferative diabetic retinopathy. In this disorder the retina becomes ischemic and releases a variety of chemical messengers, most importantly vascular endothelial growth factor (VEGF) that stimulate the growth of new blood vessels and also markedly increase retinal vascular permeability. The abnormal new vessels, and associated fibrous tissue and macular edema are major causes of the sight-threatening complications in diabetic eye disease. By destroying a portion of the peripheral retina with laser, it has been hypothesized that retinal metabolic demands and available nutrients are better balanced and the stimulus for growth of the new blood vessels is decreased. This treatment has been termed panretinal photocoagulation (PRP) and significantly reduces the risk of vision loss due to neovascularization. The side effects of panretinal photocoagulation – mild nyctalopia and constriction of visual field- are felt to be outweighed by the preservation of the central vision, and have been confirmed in multiple large randomized clinical trials[19]. Similarly, the focal laser photocoagulation to actively leaking microaneurysms, and the grid photocoagulation to areas of diffuse retinal permeability have been shown to reduce clinically significant macular edema associated with diabetic retinopathy and slow the rate of vision loss. These effects have been confirmed in large randomized multicenter clinical trials[20].

Age Related Macular Degeneration: Extrafoveal Neovascular Lesions

Another application for laser photocoagulation in the past was for the treatment of extrafoveal CNV membranes that occur in AMD. Intense photocoagulation destroyed the invading vascular membrane usually leaves a chorioretinal scar, and a blind spot or scotoma, but if the lesions treated were outside the center of the macula, the treatment was typically well tolerated by the patients. Currently, many physicians have elected to use PDT as an alternative to intense focal photocoagulation, or to use anti-VEGF therapy, because of later recurrences and eventual spread of lesions into the macula.

Additional applications of retinal photocoagulation include grid and focal treatment of leaking microvascular abnormalities, in branch-vein occlusion and radiation retinopathy; and treatment of retinal breaks and lattice degeneration to prevent retinal detachment.

Selection of optimal wavelength for coagulation

A number of important factors must be considered when choosing the best wavelength for a particular photocoagulation application. The first consideration is to determine what absorbers are present in the site to be photocoagulated. Wavelengths that are highly absorbed by macular yellow (such as 488 nm) are relatively contra-indicated when treating in or near the macula. Absorption of these wavelengths in macular pigments may cause heating and destruction of the nerve fiber layer, resulting in loss of vision. As shown in Figure 3B, in the macular region, wavelengths longer than 500 nm should be chosen, such as the green argon (514 nm) or the frequency doubled YAG (532 nm) or semiconductor yellow (577nm) laser. Melanin provides good absorption at most photocoagulation wavelengths. Wavelength selection is therefore less important when melanin is the primary absorber. To minimize scattering loss in cataract or in vitreous opacities the longer wavelengths (yellow - 577nm or red - 640 to 680 nm) are preferable. If scattering by the ocular tissues is not significant, the argon green (514nm) or doubled YAG (532nm) continue to serve well.

When hemoglobin is the primary absorber (see Figure 3B), as in the treatment of vascularized tumors, a wavelength shorter than 600 nm is preferable. Treatment of CNV may be effective using red light through indirect heat transfer from the surrounding melanin. Tunable lasers may provide the flexibility to select a wavelength of choice for required photothermal procedure. However, tunable lasers are more costly, require more maintenance, and are now less commonly employed clinically than previously.

Laser Trabeculoplasty

Argon Laser Trabeculoplasty (ALT) is usually applied to patients with open-angle glaucoma whose intraocular pressure (IOP) cannot be controlled by maximum pharmacological therapy. Safety and efficacy of ALT in treatment-naive subjects with newly diagnosed primary open-angle glaucoma has been demonstrated in large multicenter prospective clinical trial (POAG) in 1995 [21]. ALT provided longer control of intraocular pressure (IOP) without the need for additional therapy, and greater stability of visual field and optic nerve status, as compared with timolol monotherapy[22]. ALT lowers IOP by 6-10 mmHg, usually within 4-5 weeks, and lower IOP is usually maintained for several years. ALT is reported to have 70-75% success rate of clinically significant improvement.

With Argon laser (514 nm) or more recently, with the equivalent 532nm Nd:YAG laser, 50 spots of 50 μm in diameter are applied to the 180 degrees on trabecular meshwork (TM) with pulses of 100 ms in duration (Figure 9). The mechanisms of action leading to reduction in IOP are not well established. One theory is that the thermal burns created in the trabecular meshwork contract the tissue and open spaces within trabecular meshwork, thus increasing the aqueous outflow and lowering IOP. Another possible theory states that the thermal stress induced by laser therapy causes an increase in metabolic activity of the endothelial cell in the trabecular meshwork, which improves the aqueous outflow.

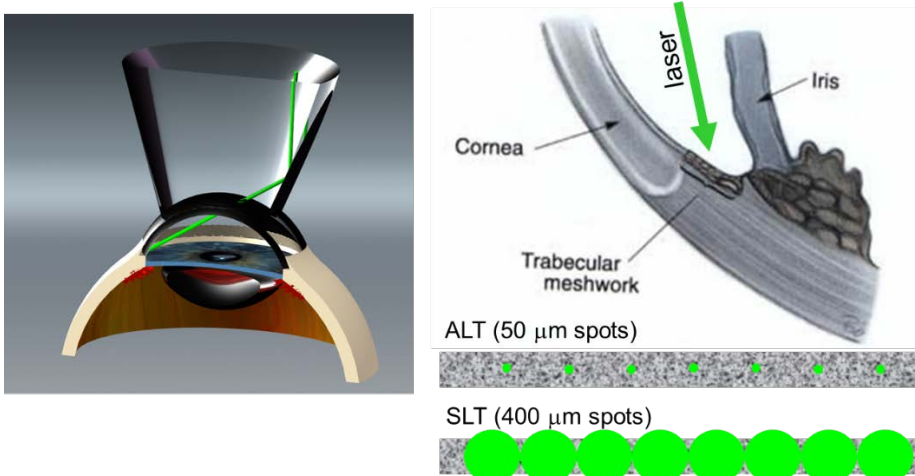


Figure 9: Laser trabeculoplasty: laser beam is directed onto the trabecular meshwork via gonioscopic lens. For ALT, laser is typically focused into 50 μm spots. For SLT, the laser spots are 400 μm in diameter.

Selective Laser Trabeculoplasty (SLT) was introduced in 1995[23, 24]. The commercially available SLT laser systems (Lumenis Inc., Santa Clara, CA; and Ellex Inc., Adelaide, Australia) include a Q-switched, frequency-doubled, 532-nm Nd:YAG laser, that delivers 3 ns pulses in a 400 μm diameter treatment spot. Typical SLT pulse energy ranges from 0.4 to 1.2 mJ, about hundred times lower than ALT. With 400 μm beam diameter, 100 spots per 360 degrees provide practically complete coverage of the TM (Figure 9). SLT has been shown to be an effective alternative to LT [23, 25, 26], in the treatment of patients with Open Angle Glaucoma. SLT leaves the Trabecular Meshwork intact with minimal damage to the endothelial cells lining the meshwork beams[23], in contrast to the ALT, which results in extensive scarring of the meshwork[27]. This observation has led to significant speculation that SLT may be more repeatable than ALT. SLT is easier to perform than ALT due to its larger spot size, and is better tolerated by patients due to reduced pulse energy. Like ALT, the IOP-lowering effect of SLT lasts for several years, but does tend to diminish over time. SLT is effective as primary therapy, can reduce the pharmaceutical burden in medically controlled eyes, and can prevent or delay the need for surgery in eyes poorly controlled, but on maximally tolerated medical therapy. Both 180 and 360-degree treatments appear to be reasonable as initial therapy, and there seems to be no contraindication to initial 360 degrees treatment.

Much lower energy requirements in SLT, compared to ALT is due to different mechanisms of cellular damage produced by nanosecond and millisecond pulses. Millisecond hyperthermia of pigmented cells leads to cellular damage due to denaturation of proteins and other cellular macromolecules[28]. Nanosecond exposures though are too short to produce thermal denaturation below the vaporization threshold, and cells are damaged by cavitation bubbles forming around melanosomes[28]. With sub-microsecond pulses the heat does not diffuse beyond one micrometer, and thus the damage can be confined within a cell. With 100 ms exposures in ALT the heat diffusion zone can reach 220 μm , covering practically the whole width of TM.

Laser Iridotomy

Laser iridotomy is performed on the eye to treat angle closure glaucoma, a condition of increased intraocular pressure caused by blockage of the angle of the anterior chamber by the iris. LI is a procedure in which the laser creates a hole in the iris to allow fluid to flow through and relieve pressure in the eye. This typically results in resolution of the forwardly bowed iris and thereby an opening up of the angle of the eye (Figure 10). It is also used prophylactically with anatomically narrow angles, in the fellow eye of a patient with primary pupil block angle closure, a patient with primary open angle glaucoma and coincidentally narrow angles, and nanophthalmos. LI is performed ~3mm from iris root under the superior lid to prevent monocular diplopia. Power and pulse duration vary with iris color of the patient. Pulses (100-300 ms) of argon laser (514nm) or 532nm YAG laser focused into 50 μm spot are applied to create a depression. A "smoke signal" is seen when the posterior pigment epithelial layer is reached. The process is continued until penetration is complete. A combination of millisecond pulses of Argon laser and nanosecond pulses of Q-switched YAG is often used to perform the procedure. The Argon is used first to initiate tissue removal and photocoagulate vessels to prevent hemorrhages and then the ns YAG is used to complete the iridotomy[29]. The ns YAG laser does not coagulate tissue, and used alone can cause hemorrhages.

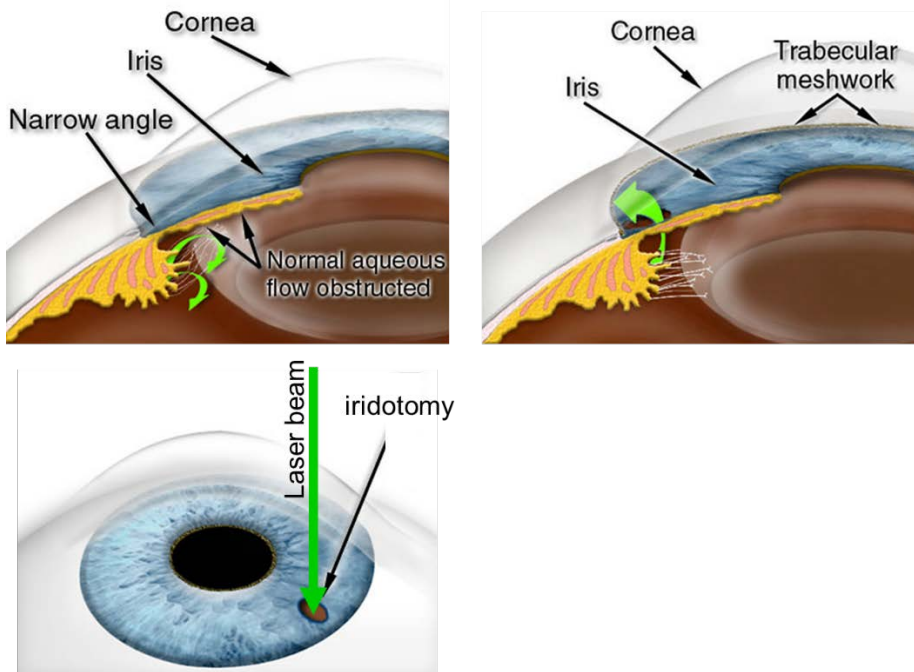


Figure 10: Laser iridotomy providing an alternative route for the aqueous flow from posterior to anterior chamber of the eye.

Posterior Capsulotomy

Posterior lens capsule opacification (PCO) is the most common late complication occurring in approximately third of the cataract surgery cases[30]. Laser is used to remove the hazy central part of the posterior capsule situated behind the intraocular lens (IOL) implant. The slit lamp-coupled nanosecond Nd:YAG laser focused into a tight spot can produce extremely high light intensities – in excess of 10^{10} W/cm². At these irradiancies photons can ionize even transparent materials via several different mechanisms[6], producing plasma in a focal spot. Plasma energy converting into heat results in rapid vaporization of the focal volume, producing shock waves and cavitation bubbles. Rapidly expanding and collapsing vapor bubbles can rupture (a process called photodisruption) the adjacent opacified posterior lens capsule, providing a clear window for central vision. To avoid damage to the intraocular lens implant, the laser is focused slightly posterior to the capsule in the vitreous (Figure 11).

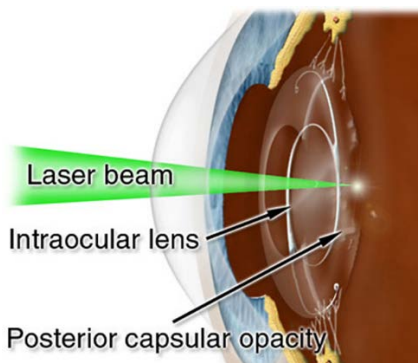


Figure 11: Laser iridotomy providing an alternative route for the aqueous flow from posterior to anterior chamber of the eye.

Refractive Surgery

Laser-Assisted In Situ Keratomileusis (LASIK) includes 2 steps: 1) cutting of a flap in the cornea (by mechanical microkeratome or a femtosecond laser) to pull it back and expose the corneal stroma for laser ablation; 2) ablation of the corneal stroma with 193nm excimer laser [31]. ArF excimer laser radiation is absorbed in a very shallow layer of the cornea (~200nm), and short pulse duration (10-20 ns) prevents heat diffusion from the light absorption zone during the pulse, by more than a few nanometers. These features enable very precise ablation of the cornea by ArF laser, ejecting the overheated surface material layer by layer, with the steps of about 200nm per pulse. Such precise tissue scalping with very shallow residual tissue damage zone allows precise reshaping of the corneal surface to correct refractive errors. After the laser reshaping of the stroma, the corneal flap is placed back over the treatment area, and its adhesion to the surrounding tissue improves over time due to natural healing.

Development of the femtosecond laser for corneal flap cutting, based on dielectric breakdown of the tissue in the tightly focused laser beam [32], enabled further improvements. Unlike mechanical microkeratome, laser cutting allowed the formation of vertical walls around the planar flap, which enabled better positioning of the corneal flap back into original location after ablation. This improved the consistency of refractive outcomes, and led to wide acceptance of the fs laser in refractive surgery[33, 34]. Ultrafast lasers also enabled refractive surgical procedures based on intrastromal cutting, without excimer laser ablation: extraction of lenticules[35] and producing pockets for intrastromal rings[36]. The same laser systems have been applied to transplantation of the whole cornea or corneal endothelium[37], so called Endothelial Keratoplasty.

In Laser Thermal Keratoplasty (LTK) long pulses of the mid-infrared laser (Holmium YAG, 2.1mm wavelength) are applied in a ring pattern of 6-7 mm in diameter. Heating of the upper third of the corneal stroma results in collagen shrinkage, thereby steepening it to correct hyperopia[38]. Similar effect can be produced by electric current, the procedure called conductive keratoplasty[39]. This effect may regress somewhat over time.

Cataract Surgery

Conventional cataract surgery involves manual formation of an opening in the anterior lens capsule, fragmentation and evacuation of the lens tissue using ultrasound probe, and implantation of a plastic intraocular lens into the remaining capsular bag. The size, shape and position of the anterior capsular opening (one of the most critical steps in the procedure) is controlled by a freehand pulling and tearing the capsular tissue. Recently developed new laser-based technique greatly improves the precision and reproducibility of cataract surgery by performing anterior capsulotomy, lens segmentation and corneal incisions with a femtosecond laser[11]. Exact placement of the cutting patterns in tissue is determined by imaging the anterior segment of the eye using integrated Optical Coherence Tomography[12], as illustrated in Figure 12. Femtosecond laser produces 3-dimensional patterns of cutting to soften the crystalline lens and to cut a round opening in the anterior capsule. Three-dimensional cutting of the cornea based on diagnostic imaging can improve safety by creating multi-planar self-sealing cataract incisions, and can reduce residual astigmatism by exact placement of the limbal relaxing incisions.

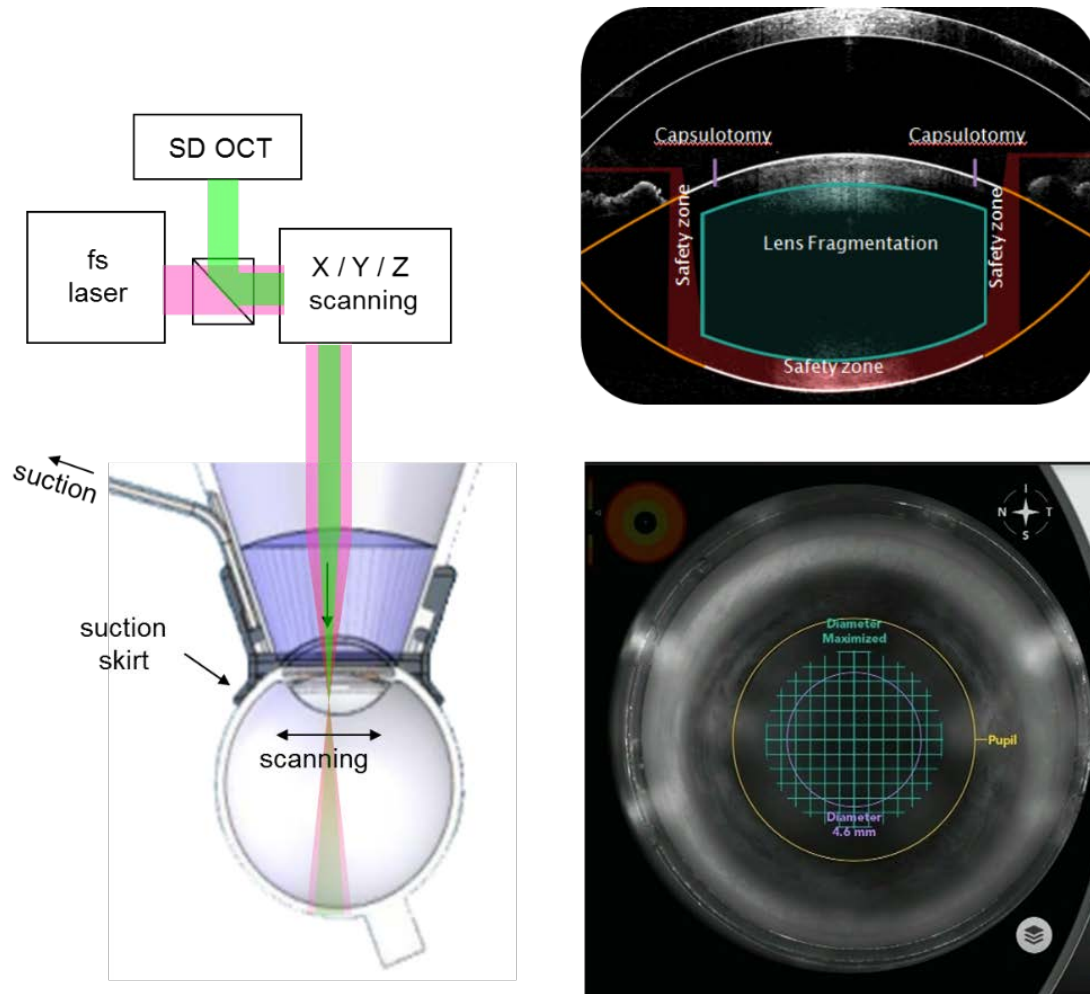


Figure 12: Left: system diagram, including the OCT and femtosecond laser combined by a common scanner. Right: Side and top views of the eye, with overlay of the planned laser patterns.

Other Procedures (less common or under investigation)

- **Anterior Stromal Puncture** for traumatic recurrent corneal erosion.
- **Laser Suture Lysis** for post-filtration or cataract surgery.
- **Oculoplastic Surgery** (CO₂ or Argon laser): port-wine stain, capillary hemangioma, basal cell carcinoma, trichiasis, xanthelasma, phthiriasis palpebrarum.
- **Photomydriasis** (to enlarge pupil)
- **Anterior Synechiolysis** for iris incarceration, adhesions involving anterior and posterior capsule, and vitreous body strands.

References

1. Kramer, M., et al., *Liposomal benzoporphyrin derivative verteporfin photodynamic therapy. Selective treatment of choroidal neovascularization in monkeys.* Ophthalmology, 1996. **103**(3): p. 427-38.
2. Schmidt-Erfurth, U., et al., *Photodynamic therapy of subfoveal choroidal neovascularization: clinical and angiographic examples.* Graefes Arch Clin Exp Ophthalmol, 1998. **236**(5): p. 365-74.
3. Woodburn, K.W., C.J. Engelman, and M.S. Blumenkranz, *Photodynamic therapy for choroidal neovascularization: a review.* Retina, 2002. **22**(4): p. 391-405; quiz 527-8.
4. Sramek, C., et al., *Dynamics of Retinal Photocoagulation and Rupture.* J. Biomedical Optics, 2009. **14**(3): p. 034007-1-13.
5. Simanovskii, D.M., et al., *Cellular tolerance to pulsed hyperthermia.* Phys Rev E Stat Nonlin Soft Matter Phys, 2006. **74**(1 Pt 1): p. 011915.
6. Vogel, A. and V. Venugopalan, *Mechanisms of pulsed laser ablation of biological tissues (vol 103, pg 577, 2003).* Chemical Reviews, 2003. **103**(5): p. 2079-2079.

7. Vogel, A., et al., *Mechanisms of intraocular photodisruption with picosecond and nanosecond laser pulses*. *Lasers Surg Med*, 1994. **15**(1): p. 32-43.
8. Krueger, R.R., et al., *Ultrastructure of picosecond laser intrastromal photodisruption*. *Journal of Refractive Surgery*, 1996. **12**(5): p. 607-612.
9. Yen, K.G., et al., *Histopathology of femtosecond laser intrastromal refractive surgery in rabbits*. *Investigative Ophthalmology & Visual Science*, 1999. **40**(4): p. S621-S621.
10. Cohen, B.Z., K.J. Wald, and K. Toyama, *Neodymium:YLF picosecond laser segmentation for retinal traction associated with proliferative diabetic retinopathy*. *American Journal of Ophthalmology*, 1997. **123**(4): p. 515-523.
11. Palanker, D.V., et al., *Femtosecond laser-assisted cataract surgery with integrated optical coherence tomography*. *Sci Transl Med*, 2010. **2**(58): p. 58ra85.
12. Friedman, N.J., et al., *Femtosecond laser capsulotomy*. *J Cataract Refract Surg*, 2011. **37**(7): p. 1189-98.
13. Wright, C.H.G., et al., *Initial in vivo results of a hybrid retinal photocoagulation system*. *Journal of Biomedical Optics*, 2000. **5**(1): p. 56-61.
14. Blumenkranz, M.S., et al., *Semiautomated patterned scanning laser for retinal photocoagulation*. *Retina-the Journal of Retinal and Vitreous Diseases*, 2006. **26**(3): p. 370-376.
15. Nagpal, M., S. Marlecha, and K. Nagpal, *Comparison of laser photocoagulation for diabetic retinopathy using 532-nm standard laser versus multispot pattern scan laser*. *Retina*, 2010. **30**(3): p. 452-8.
16. Muqit, M.M., et al., *Pain responses of Pascal 20 ms multi-spot and 100 ms single-spot panretinal photocoagulation: Manchester Pascal Study, MAPASS report 2*. *Br J Ophthalmol*, 2010. **94**(11): p. 1493-8.
17. Muqit, M.M., et al., *In vivo laser-tissue interactions and healing responses from 20- vs 100-millisecond pulse Pascal photocoagulation burns*. *Arch Ophthalmol*, 2010. **128**(4): p. 448-55.
18. Palanker, D., et al., *THE IMPACT OF PULSE DURATION AND BURN GRADE ON SIZE OF RETINAL PHOTOCOAGULATION LESION: Implications for Pattern Density*. *Retina*, 2011.
19. DRS_Study_Group, *Photocoagulation Treatment for Proliferative Diabetic Retinopathy. Clinicial Application of DRS findings, DRS Report Number 8*. *Ophthalmology*, 1981. **88**: p. 583-600.
20. ETDRS_Study_Group, *Early Photocoagulation for Diabetic Retinopathy. ETDRS Report Number 9*. *Ophthalmology*, 1991. **98**: p. 766-785.
21. *The Glaucoma Laser Trial (GLT) and glaucoma laser trial follow-up study: 7. Results*. *Glaucoma Laser Trial Research Group*. *Am J Ophthalmol*, 1995. **120**(6): p. 718-31.
22. Kass, M.A., et al., *The Ocular Hypertension Treatment Study: a randomized trial determines that topical ocular hypotensive medication delays or prevents the onset of primary open-angle glaucoma*. *Arch Ophthalmol*, 2002. **120**(6): p. 701-13; discussion 829-30.
23. Latina, M.A., et al., *Q-switched 532-nm Nd:YAG laser trabeculoplasty (selective laser trabeculoplasty): a multicenter, pilot, clinical study*. *Ophthalmology*, 1998. **105**(11): p. 2082-8; discussion 2089-90.
24. Latina, M.A. and C. Park, *Selective targeting of trabecular meshwork cells: in vitro studies of pulsed and CW laser interactions*. *Exp Eye Res*, 1995. **60**(4): p. 359-71.
25. Nagar, M., et al., *A randomised, prospective study comparing selective laser trabeculoplasty with latanoprost for the control of intraocular pressure in ocular hypertension and open angle glaucoma*. *Br J Ophthalmol*, 2005. **89**(11): p. 1413-7.
26. Melamed, S., G.J. Ben Simon, and H. Levkovitch-Verbin, *Selective laser trabeculoplasty as primary treatment for open-angle glaucoma: a prospective, nonrandomized pilot study*. *Arch Ophthalmol*, 2003. **121**(7): p. 957-60.
27. Wise, J.B. and S.L. Witter, *Argon laser therapy for open-angle glaucoma. A pilot study*. *Arch Ophthalmol*, 1979. **97**(2): p. 319-22.
28. Schuele, G., et al., *RPE damage thresholds and mechanisms for laser exposure in the microsecond-to-millisecond time regimen*. *Invest Ophthalmol Vis Sci*, 2005. **46**(2): p. 714-9.
29. He, M., et al., *Laser peripheral iridotomy in primary angle-closure suspects: biometric and gonioscopic outcomes: the Liwan Eye Study*. *Ophthalmology*, 2007. **114**(3): p. 494-500.
30. Apple, D.J., et al., *Posterior capsule opacification*. *Surv Ophthalmol*, 1992. **37**(2): p. 73-116.
31. Pallikaris, I.G., et al., *A corneal flap technique for laser in situ keratomileusis. Human studies*. *Arch Ophthalmol*, 1991. **109**(12): p. 1699-702.
32. Kurtz, R.M., et al., *Lamellar refractive surgery with scanned intrastromal picosecond and femtosecond laser pulses in animal eyes*. *Journal of Refractive Surgery*, 1998. **14**(5): p. 541-8.
33. Ratkay-Traub, I., et al., *Ultra-short pulse (femtosecond) laser surgery: initial use in LASIK flap creation*. *Ophthalmol Clin North Am*, 2001. **14**(2): p. 347-55, viii-ix.
34. Nordan, L.T., et al., *Femtosecond laser flap creation for laser in situ keratomileusis: six-month follow-up of initial U.S. clinical series*. *J Refract Surg*, 2003. **19**(1): p. 8-14.
35. Heisterkamp, A., et al., *Photodisruption with ultrashort laser pulses for intrastromal refractive surgery*. *Laser Physics*, 2003. **13**(5): p. 743-748.
36. Ertan, A. and M. Bahadir, *Intrastromal ring segment insertion using a femtosecond laser to correct pellucid marginal corneal degeneration*. *J Cataract Refract Surg*, 2006. **32**(10): p. 1710-6.

37. Jonas, J.B., *Corneal endothelial transplantation using femtosecond laser technology*. Eye, 2004. **18**(6): p. 657-658.
38. Ariyasu, R.G., et al., *Holmium laser thermal keratoplasty of 10 poorly sighted eyes*. J Refract Surg, 1995. **11**(5): p. 358-65.
39. Haw, W.W. and E.E. Manche, *Conductive keratoplasty and laser thermal keratoplasty*. Int Ophthalmol Clin, 2002. **42**(4): p. 99-106.